

## General Disclaimer

### One or more of the Following Statements may affect this Document

- This document has been reproduced from the best copy furnished by the organizational source. It is being released in the interest of making available as much information as possible.
- This document may contain data, which exceeds the sheet parameters. It was furnished in this condition by the organizational source and is the best copy available.
- This document may contain tone-on-tone or color graphs, charts and/or pictures, which have been reproduced in black and white.
- This document is paginated as submitted by the original source.
- Portions of this document are not fully legible due to the historical nature of some of the material. However, it is the best reproduction available from the original submission.

X-693-75-156

PREPRINT

NASA TM X-70945

**OBSERVATIONS OF MAGNETOSPHERIC  
IONIZATION ENHANCEMENTS USING  
UPPER-HYBRID RESONANCE NOISE  
BAND DATA FROM THE RAE-1 SATELLITE**

(NASA-TM-X-70945) OBSERVATIONS OF  
MAGNETOSPHERIC IONIZATION ENHANCEMENTS USING  
UPPER-HYBRID RESONANCE NOISE BAND DATA FROM  
THE RAE-1 SATELLITE (NASA) 19 p HC \$3.25

N75-30994

Unclas

CSCI 03B G3/93 34749

**STEPHEN R. MOSIER**

**AUGUST 1975**



**GODDARD SPACE FLIGHT CENTER  
GREENBELT, MARYLAND**

OBSERVATIONS OF MAGNETOSPHERIC IONIZATION  
ENHANCEMENTS USING UPPER-HYBRID  
RESONANCE NOISE BAND DATA  
FROM THE RAE 1 SATELLITE

Stephen R. Mosier

Radio Astronomy Branch  
Laboratory for Extraterrestrial Physics  
NASA/Goddard Space Flight Center  
Greenbelt, MD 20771

## ABSTRACT

Noise bands associated with the upper-hybrid resonance have been used to provide direct evidence for the existence of regions of enhanced density in the equatorial magnetosphere near  $L = 2$ . Density enhancements ranging from several percent to as high as 45 percent are observed with radial dimensions of several hundred kilometers. The enhancement characteristics strongly suggest their identification as magnetospheric whistler ducts.

Whistler studies from both ground stations and spacecraft have long indicated the existence of magnetospheric ducts of enhanced density which guide whistler waves between conjugate hemispheres. The first evidence from spacecraft data that such ducts actually exist was derived from OGO 1 data by Smith and Angerami [1968]. A more detailed analysis of data from OGO 3 was performed by Angerami [1970] in which estimates of the L-shell thicknesses, elongation in longitude, and enhancement magnitudes for ducts were obtained from whistler observations between  $L = 4.1$  and  $L = 4.7$ . Cerisier [1974] observed ducted waves together with the irregularity responsible for the ducting, using data from the FR 1 satellite at 750 km altitude. However, at magnetospheric altitudes, there has been no direct measurement of the relative density variations through a duct region. This paper reports on the observations of ionization enhancements with the RAE 1 satellite at L-values near 2 at the equator, using observations of noise bands associated with the upper-hybrid resonance to measure the relative density fluctuations at the satellite. These enhancements have the same characteristic dimensions and magnitudes as those inferred from the study of whistler ducting, thereby supporting the existence of whistler ducts of enhanced ionization.

Observations of noise band phenomena occurring below the upper-hybrid resonance (UHR) frequency and extending below the local

electron plasma frequency have been reported by several investigators.

The UHR frequency is given by the relation

$$\omega_{\text{UHR}}^2 = \omega_{\text{pe}}^2 + \omega_{\text{ge}}^2, \quad (1)$$

where  $\omega_{\text{UHR}}$  is the angular UHR frequency,  $\omega_{\text{pe}} = (4\pi ne^2/m)^{1/2}$  is the angular electron plasma frequency,  $\omega_{\text{ge}} = eB/mc$  is the angular electron cyclotron frequency,  $n$  is local electron density,  $m$  is electron mass,  $e$  is electronic charge, and  $B$  is geomagnetic field strength (gaussian units are used). The most characteristic feature of these naturally occurring noise bands is the sharp onset at, or just below, the local UHR frequency.

This study utilizes observations of noise bands associated with the UHR at frequencies of 540 and 700 kHz. At the orbit of RAE 1, the local UHR frequency occurs between these two frequencies as the satellite traverses the equatorial region. Fine structure anticorrelations of intensity between these two observing frequencies are observed over short spatial distances and may be interpreted as local density inhomogeneities along the satellite path. This paper discusses the interpretation of the noise bands in terms of such inhomogeneities, or ducts, and the implications of the required scale sizes and magnitudes.

## INSTRUMENTATION

The Radio Astronomy Explorer (RAE 1) satellite was launched on 4 July 1968 into a 5850-km circular Earth orbit of 121-degree (retrograde) inclination. The instrumentation was designed to measure long-wavelength radio phenomena emitted from the magnetosphere, the solar corona and the Galaxy. The data used in this study were acquired by fixed-frequency total power radiometers and a 37-meter tip-to-tip electric dipole antenna; frequencies of 540 and 700 kHz were chosen because of their relation to the UHR frequency at the equator. Additional data from a step-frequency radiometer were used as an independent system for establishing a local density scale from UHR noise bands using the method discussed by Mosier et al. [1973], hereafter referred to as Paper I. The spacecraft utilizes gravity gradient stabilization and gyroscopic forces maintain the dipole antenna alignment to within 13 degrees of the satellite velocity vector. A detailed description of the RAE 1 satellite is given by Weber et al. [1971].

## OBSERVATIONS

Figure 1 is a plot of the 540- and 700-kHz noise intensities for an equatorial transit by the spacecraft. The basic features observed on most such transits are the two noise bands at 540 kHz occurring on either side of the dipole equator and the single noise band at

700 kHz centered approximately at the equator. A self-consistent fit of a local electron density scale to the characteristic frequencies in the plasma was obtained by using noise band observations at several closely-spaced frequencies (see Paper I). Then, using computed values of the geomagnetic field strength, the spacecraft orbit was plotted on a CMA diagram [Ratcliffe, 1962] (also in Figure 1). In this diagram, scale lengths in the abscissa and ordinate are proportional to electron density and to the square of the magnetic field strength, respectively. Characteristic frequencies are represented by boundaries in this two-dimensional parameter space. As the spacecraft encounters increasing density it crosses the cutoff for the x-wave of the extraordinary mode ( $R = 0$  in the notation of Stix [1962]), the upper-hybrid resonance ( $S = 0$ ), the electron plasma frequency ( $P = 0$ ) and the cutoff for the z-wave of the extraordinary mode ( $L = 0$ ), where

$$R \equiv 1 - \frac{\omega_{pe}^2}{\omega(\omega - \omega_{ge})} \quad (2)$$

$$L \equiv 1 - \frac{\omega_{pe}^2}{\omega(\omega + \omega_{ge})} \quad (3)$$

$$S \equiv \frac{1}{2}(R + L) = 1 - \frac{\omega_{pe}^2}{\omega^2 - \omega_{ge}^2} \quad (4)$$

$$P \equiv 1 - \frac{\omega_{pe}^2}{\omega} \quad (5)$$



For a discussion of the x- and z-wave notation commonly used in ionospheric physics, see Ratcliffe [1962]. (The z-wave cutoff, defined by  $L = O$ , should not be confused with McIlwain's [1961] geomagnetic shell parameter  $L$ , discussed earlier). The four boundaries define five regions on the CMA diagram of Figure 1, numbered from left to right.

As reported in Paper I, a noise-intensity increase of 10 to 20 dB is often observed between  $R = O$  and  $S = O$  (region 2). The most intense noise bands (30 to 40 dB above background) were observed in regions 3 and 4. Background intensity is not always attained by the time the spacecraft reaches region 5 and there is often a further intensity decrease of approximately 10 dB beyond  $L = O$ . When the noise intensity at 540 and 700 kHz in Figure 1 exceeded a threshold of 10 dB above background (indicated by horizontal bars under the noise plots), the CMA orbit in Figure 1 is plotted as a heavy line. The most intense noise thus occurs in a band from about  $f_z$  to  $f_{UHR}$ . This noise band appears in the two channels sequentially as the spacecraft traverses a smoothly varying plasma. In regions of the orbit where the noise band appears only in the lower channel, an anomalous increase in plasma density, if sufficiently large, can displace the noise band out of the lower channel and into the upper one. Similarly, anomalous decreases would be detectable in those regions

where the noise appears only in the upper channel. In reality, both enhancements and depressions are detectable in either region, but the confidence level is low for the two cases not discussed above since a signature would be present in only one channel. However, the absence of the necessary signature is sufficient proof that a large inhomogeneity is not present. Typical inhomogeneity signatures are seen in Figure 2, where an increase in noise intensity at one frequency is accompanied by a simultaneous decrease in intensity at the other frequency. These anticorrelated intensity features track quite well as seen in Figure 3, where a single feature (on a different date) is shown at increased resolution. At 2228:10 UT in Figure 3, the 540-kHz noise intensity increases 26 dB in 13 sec, accompanied by a 21-dB decrease at 700 kHz at the same time. In 12 sec, the spacecraft travels 74 km. The duration of the "event" in Figure 3 is two minutes, during which the spacecraft travels 685 km.

The choice of the 540- and 700-kHz observing frequencies limits the observation of UHR noise to within approximately 30 to 40 degrees of the geomagnetic equator. The anticorrelated fine-structure intensity features are observed throughout this region and at all local times. Assuming that the observed inhomogeneities are the signatures of magnetospheric propagation ducts, then these data are in good agreement with Cerisier [1974] who found that ducted propagation

is a quasi-permanent feature of the VLF field between  $L = 1.7$  and 3. The RAE 1 observations were strongly grouped at low values of the geomagnetic activity  $K_p$  index. This is probably due to the selection of data during periods of low background noise activity for ease in determining local density scales and does not necessarily reflect a correlation of the fine structure with low values of  $K_p$ .

## DISCUSSION

From a study of the typical noise intensities observed in the different CMA regions [Paper I], we conclude that when either the 540- or 700-kHz intense noise (i.e., 20 to 30 dB above background) is cutoff, the observation cannot lie in region 3 or 4. Therefore, at the onset of the event in Figure 3, the reduction of the 540-kHz signal and the onset of the 700-kHz signal must correspond to a sudden increase in electron density (a shift from region 3 or 4 to region 5 along the solid line orbital track and a shift from region 1 or 2 to region 3 or 4 along the dashed line orbital track on the CMA diagram in Figure 1). Using noise resonance data at several other frequencies combined with the RAE 1 capacitance probe data, a value of 25 percent has been derived for the minimum density enhancement required to explain the structure in Figure 3. This minimum value reflects uncertainties in the ambient density determination and allows for a possibly greater enhancement magnitude. In defining the enhancement magnitude,

the highest density attained is that which shifts the 700-kHz orbit plot into region 3. The background density from which the enhancement is measured is dependent upon the position of the orbit plot for the 700-kHz background noise intensity. In order to better define the enhancement magnitudes, a study of 244 cases was performed using UHR noise band data and the dipole antenna capacitance probe on RAE 1 to determine the local electron density for each event just before the onset of intense noise at 700 kHz. The resulting data must be treated statistically due to the uncertainty associated with density determinations by capacitance probe techniques (for a discussion of the calibration of the RAE 1 capacitance probe using UHR noise bands, see Mosier and Kaiser [1975]). From a preliminary statistical study of these data, it appears that the observed density enhancement magnitudes range from less than 10 to 15 percent to as great as 45 percent. These enhancements occur typically within cross-L-shell distances of the order of hundreds of kilometers. The suggested geometry of the density enhancement in relation to the satellite trajectory is shown in Figure 4.

The physical picture shown in Figure 4 which we derive from the data is of a field-aligned ionization enhancement, or duct, of as much as 45 percent of the ambient density and of several hundred

kilometers spatial extent radially at the equator near  $L = 2$  at all local times. This is in good agreement with Angerami [ 1970 ] , who derived duct thicknesses of 220 to 430 km radially at the equator near  $L = 4$  from whistler observations with OGO 3.

Furthermore, the UHR data present evidence to support the long-standing hypothesis that whistler ducts are enhancements, rather than depressions, of ionization. Although some density depressions are observed, they are generally of much smaller magnitude than are the enhancements and are quite often superimposed on enhanced density levels; dramatic depressions of density have seldom been observed. Using a model for whistler ducting, Angerami [ 1970 ] concluded that the minimum density enhancement required for supporting guided whistlers is between 4 and 8 percent. He further estimated that enhancements generally lie between 6 and 22 percent and rarely exceed 33 percent. The UHR data reported here confirm Angerami's estimates but extend the upper limit of enhancement magnitude to over 40 percent.

Park and Helliwell [ 1971 ] suggested a possible mechanism to explain irregularities in electron density involving  $\underline{E} \times \underline{B}$  convection cells in which tubes of ionization are mixed. They showed that a 0.1 mV/m electric field in the equatorial plane can produce electron

density enhancements and depressions of the order of 5 percent at  $L = 4$  in about one-half hour. In about one hour, multiple peaks and valleys start to appear, and at later times the scale size of the irregularities decreases and the amplitude increases slightly to near 10 percent, with dimensions between peaks and valleys of the order of 50 km. It is interesting to note from Figure 3 that there is considerable structure within the density enhancement region as observed by RAE 1. The cross-L-shell dimensions for individual structures within this region are of the order of tens of kilometers, which are consistent with the E X B convection model of Park and Helliwell [1971]. However, the RAE-1 data do not support the existence of density depressions and enhancements of equal magnitude, large depressions being rarely observed. It is possible that an electric-field-driven mechanism such as that of Park and Helliwell is operating at the RAE 1 orbit but, if so, it must certainly be a minor effect.

In summary, regions of enhanced density are observed between  $L = 1.9$  and  $L = 2.5$  within 30 degrees of the geomagnetic equator. The peak fractional density increases range from a few percent to as much as 45 percent of the normal ambient density and the structures have overall radial dimensions of several hundred kilometers, with smaller structure observed over distances of the order of tens of kilometers. The similarity of these enhancements to those derived from whistler data suggests their identity as whistler ducts.

## REFERENCES

- Angerami, J.J., Whistler duct properties deduced from VLF observations made with the OGO 3 satellite near the magnetic equator, J. Geophys. Res., 75, 6115-6135, 1970.
- Cerisier, J.C., Ducted and partly ducted propagation of VLF waves through the magnetosphere, J. Atmos. Terr. Phys., 36, 1443-1467, 1974.
- McIlwain, C.E., Coordinates for mapping the distribution of magnetically trapped particles, J. Geophys. Res., 66, 3681-3691, 1961.
- Mosier, S.R., and M.L. Kaiser, Calibration of a cylindrical RF capacitance probe, J. Geophys. Res., 80, 702-703, 1975.
- Mosier, S.R., M.L. Kaiser and L.W. Brown, Observations of noise bands associated with the upper hybrid resonance by the IMP 6 radio astronomy experiment, J. Geophys. Res., 78, 1673-1679, 1973.
- Park, C.G. and R.A. Helliwell, The formation by electric fields of field-aligned irregularities in the magnetosphere, Radio Sci., 6, 299-304, 1971.
- Ratcliffe, J.A., The Magneto-ionic Theory and Its Application to the Ionosphere, p. 59, Cambridge University Press, London, 1962.
- Smith, R.L., and J.J. Angerami, Magnetospheric properties deduced from OGO 1 observations of ducted and nonducted whistlers, J. Geophys. Res., 73, 1-20, 1968.

Stix, T.H., The Theory of Plasma Waves, pp. 27 ff, McGraw Hill, New York, 1962.

Weber, R.R., J.K. Alexander, and R.G. Stone, The Radio Astronomy Explorer satellite, a low-frequency observatory, Radio Sci., 6, 1085, 1971.



## FIGURE CAPTIONS

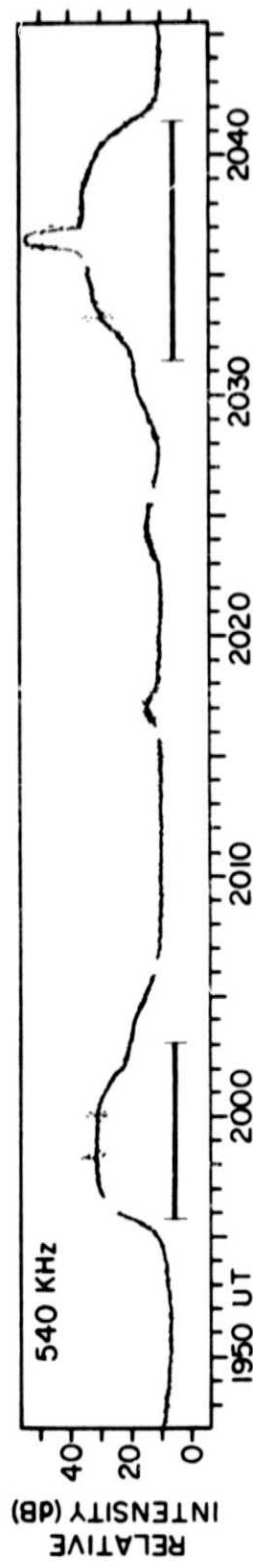
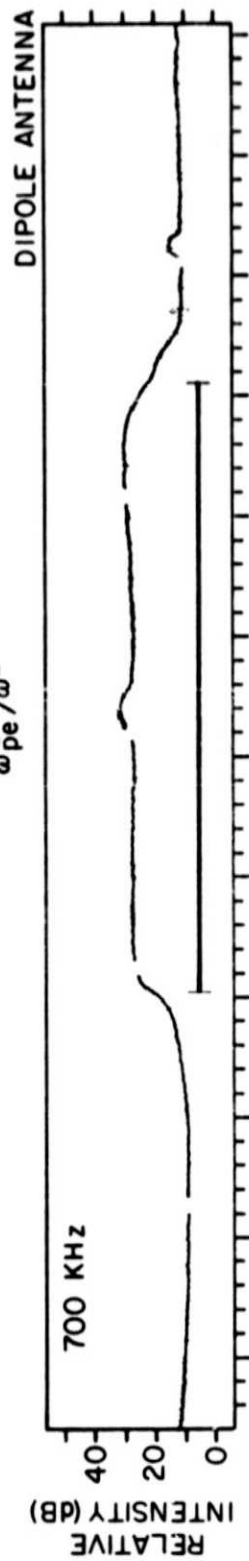
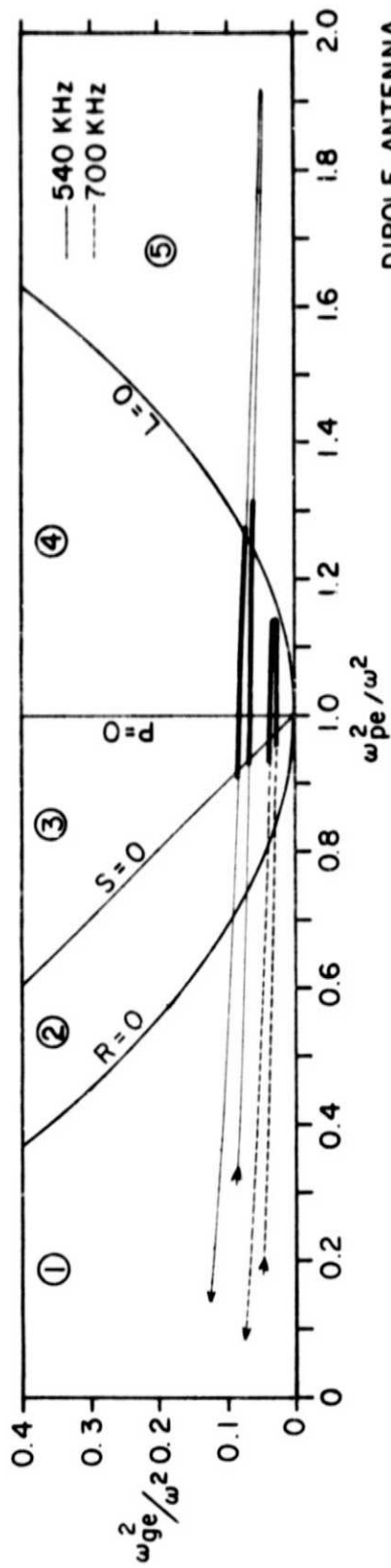
Figure 1 - UHR noise bands observed at 540 and 700 kHz and the CMA diagram orbit plots for these frequencies. The horizontal bars under the noise peaks indicate those times for which the noise intensity exceeds 10 dB above background. The CMA orbit for these times is plotted as a heavy line.

Figure 2 - UHR noise bands with superimposed anticorrelated intensity structure.

Figure 3 - Detail of anticorrelated intensity structure.

Figure 4 - Geometry of density enhancement region in relation to satellite trajectory.

# RAE-1



DIPOLE LATITUDE -25.06°      3.79°      31.74°  
 MAGNETIC LOCAL TIME 17.80 HRS      16.40 HRS      14.93 HRS

25 OCTOBER 1968

Figure 1

RAE-1

28 MAY 1969

DIPOLE ANTENNA

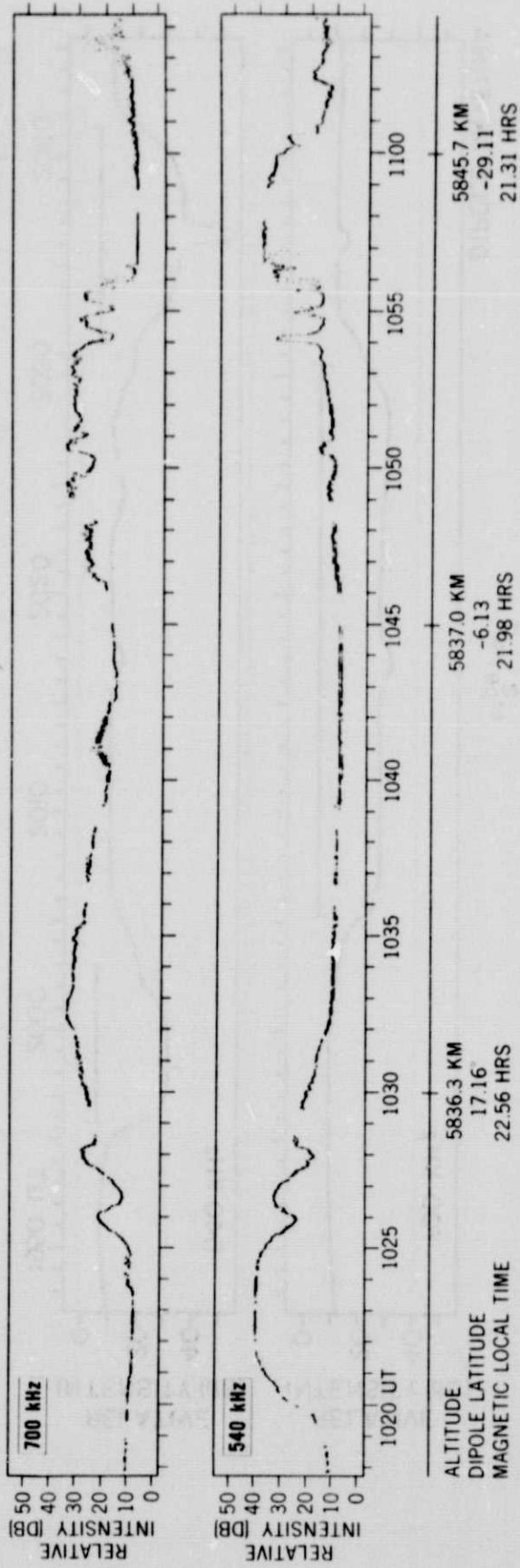


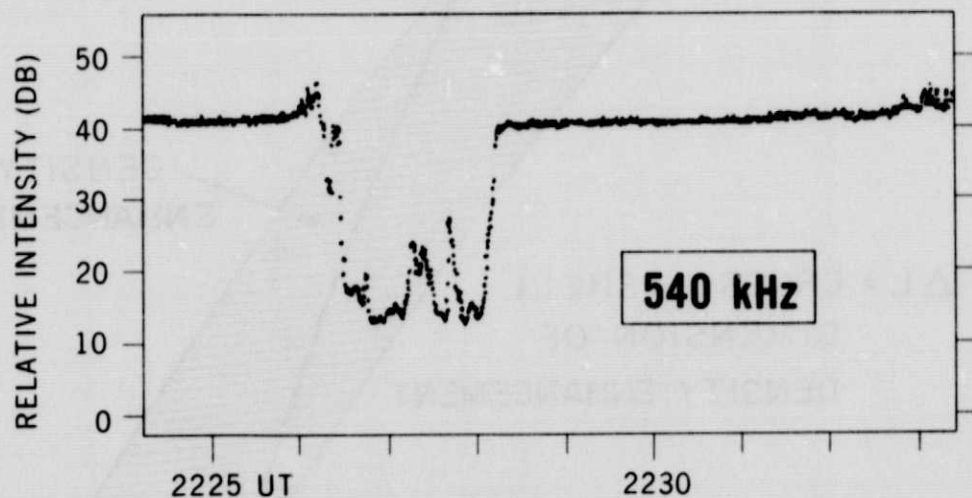
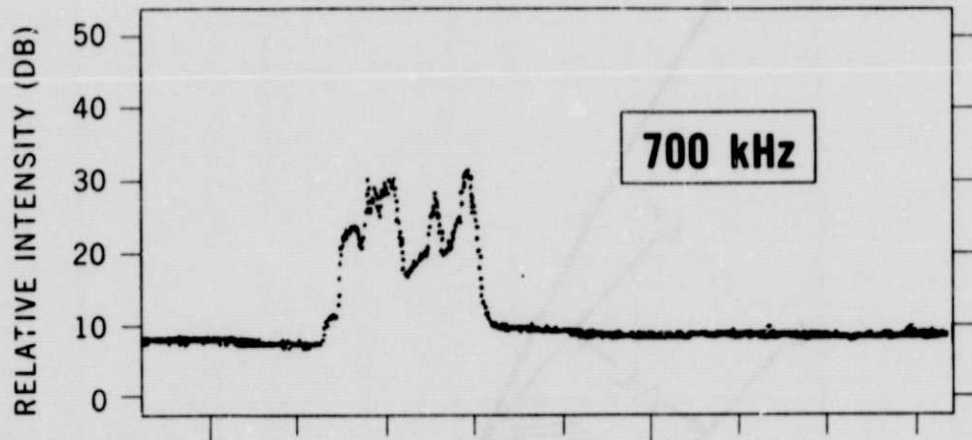
Figure 2

ORIGINAL PAGE IS  
OF POOR QUALITY

# RAE - 1

## 6 JULY 1969

DIPOLE ANTENNA



|                     |           |           |
|---------------------|-----------|-----------|
| ALTITUDE            | 5872.7 km | 5870.7 km |
| DIPOLE LATITUDE     | -17.29°   | -11.29°   |
| MAGNETIC LOCAL TIME | 9.47 hrs  | 9.11 hrs  |

Figure 3

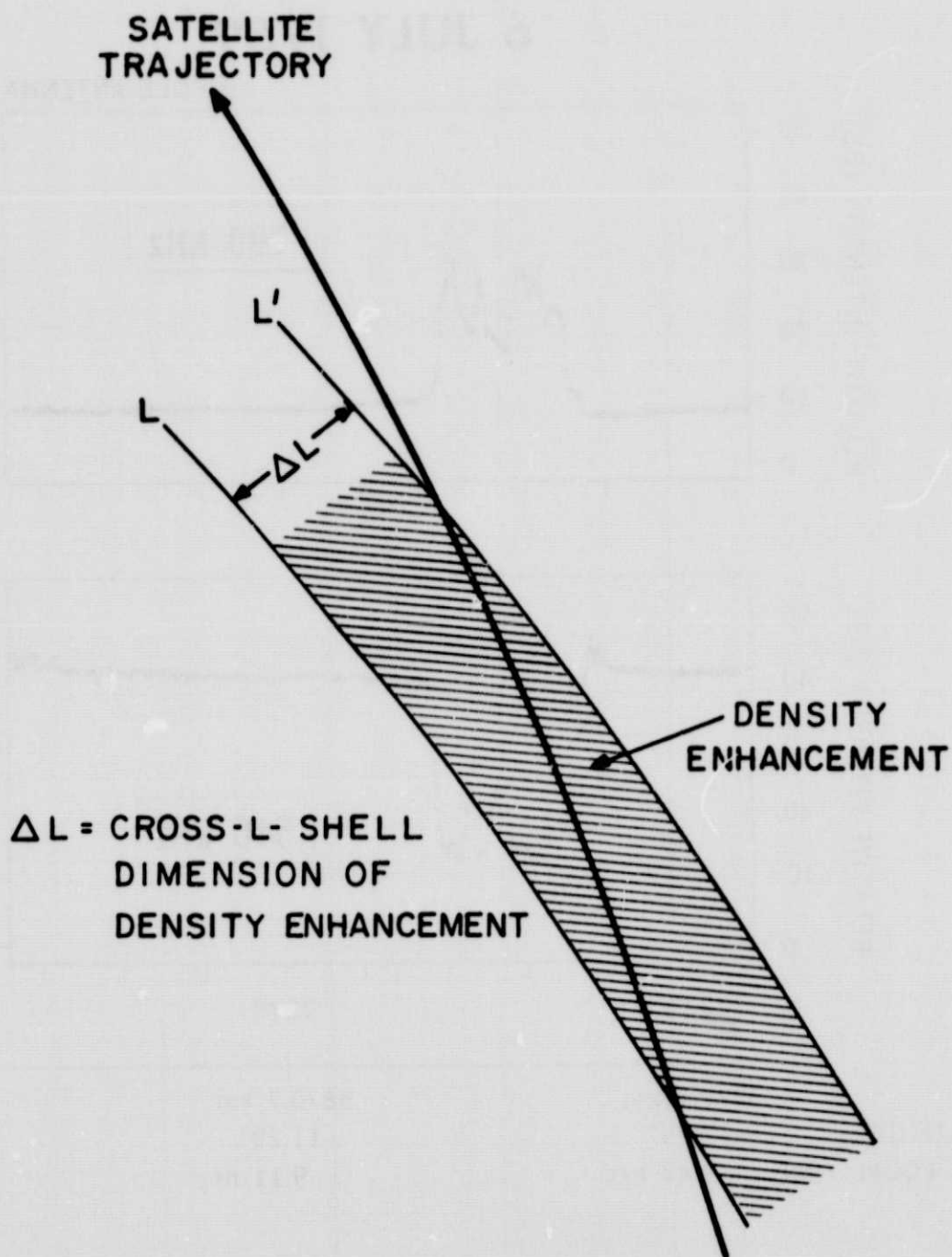


Figure 4